JAAS

ROYAL SOCIETY OF CHEMISTRY

PAPER

View Article Online
View Journal | View Issue

Cite this: *J. Anal. At. Spectrom.*, 2025, **40**, 2150

Development of a HPIC-ICP-MS method for the quantification and speciation of gadolinium-based contrast media in surface waters†

Manon Dalla Costa,[a] David Dumoulin, *[a] Marie Lenski, [bc] Anne Garat[bde] and Gabriel Billon[a]

Over the last few decades, numerous speciation methods involving hyphenated ICP-MS strategies have been developed to study gadolinium-based contrast agents (GBCAs), whose concentrations are steadily increasing in surface water in France, Europe and around the world. Most of these methods involve the extensive use of organic solvents and often require the use of an additional aerosol desolvation module. Here, a new sensitive chromatographic method has been developed to study the speciation of the six GBCAs currently marketed in France (*i.e.* Gd-DOTA, Gd-BT-DO3A, Gd-HP-DO3A, Gd-DTPA-BMA, Gd-DTPA and Gd-BOPTA). This HPIC-ICP-MS method, involving the use of an anion-exchange column, allows the separation of the charged GBCAs in less than 15 min, while using only 2% of methanol in the eluent and a standard ICP-Q-MS configuration. The detection limits obtained, ranging from 2 to 5 ng_{Gd} L^{-1}, are comparable to reference methods in the literature and are therefore well suited to environmental studies. An environmental application has been successfully carried out on water samples from the Marque River (Northern France), which is affected by the presence of numerous WWTPs. This application highlights the fact that GBCAs account for over 90% of Gd pollution in river water.

Received 20th May 2025
Accepted 19th June 2025

DOI: 10.1039/d5ja00203f

rsc.li/jaas

1. Introduction

Rare earth elements (REEs) are a family of elements corresponding to the 15 lanthanides, ranging from lanthanum (La, $Z = 57$) to lutetium (Lu, $Z = 71$), as well as scandium and yttrium. With the exception of cerium and europium, REEs are mostly found in the +III oxidation state.[1–3] These elements are found in abundance in the mantle of the Earth's crust, with concentrations ranging from a few mg kg^{-1} to several tens of mg kg^{-1}.[4–6] REEs are used in many fields, including metallurgy, ceramics and catalysis, as well as in the design of batteries, glass and magnets.[1,2,6] Increasing improvements in new technologies are also leading to the growing use of these REEs, particularly in rechargeable batteries and catalytic converters.[1,7,8] Several studies show that global REE consumption is set to increase by around 150% by 2030.[8,9] Unfortunately, this increase in the extraction and use of rare earths has, for decades, resulted in an increased presence of positive anomalies in the levels of these elements in the environment, particularly in surface waters.[1,4,6,10–13]

In the case of gadolinium (Gd, $Z = 64$), positive anomalies have been observed in France and Europe with proportions of anthropogenic Gd up to 45 to 100% of total Gd.[4,12,14–18] Like other REEs, Gd has a number of industrial applications in the nuclear, metallurgy, electronics, information technologies and medical sectors.[19,20] In this latter field, Gd has been extensively used as a contrast agent in magnetic resonance imaging examinations in France since 1988.[6,19] Gadolinium-based contrast agents (GBCAs) are organometallic complexes composed of a Gd^{3+} ion and a ligand, which may be structured in a linear or macrocyclic complex. In France, six GBCAs are marketed, with sales set to reach 2.5 million boxes a year by 2023 (Fig. 1). Since 2017, the European Medicines Agency (EMA) has suspended the marketing or limited the use of certain linear GBCAs. As a result, macrocyclic complexes now account for 99% of GBCAs marketed in France, according to data from Ameli,[20] the French health insurance (data from 2023).

Over the last few decades, the increasing use of GBCAs has led to an increase in their concentrations in surface waters, ranging from ng L^{-1} to µg L^{-1} in France and worldwide.[14,15,18,19,21,22] In addition, these compounds are hardly degraded during the conventional treatment stages of wastewater treatment plants (WWTPs), and end up in the discharge from these plants and subsequently in surface waters.[23–27]

[a]*Univ. Lille, CNRS, UMR 8516 – LASIRE, F-59000 Lille, France. E-mail: david.dumoulin@univ-lille.fr*

[b]*Univ. Lille, CHU Lille, Institut Pasteur de Lille, ULR 4483-IMPacts de l'Environnement Chimique sur la Santé (IMPECS), F-59000 Lille, France*

[c]*CHU Lille, Unité Fonctionnelle de Toxicologie, F-59037 Lille, France*

[d]*Univ. Lille, UFR3S, Département de Pharmacie, Service de Toxicologie et de Santé Publique, 59000 Lille, France*

[e]*Centre Antipoison des Hauts de France, 59000 Lille, France*

† Electronic supplementary information (ESI) available. See DOI: https://doi.org/10.1039/d5ja00203f

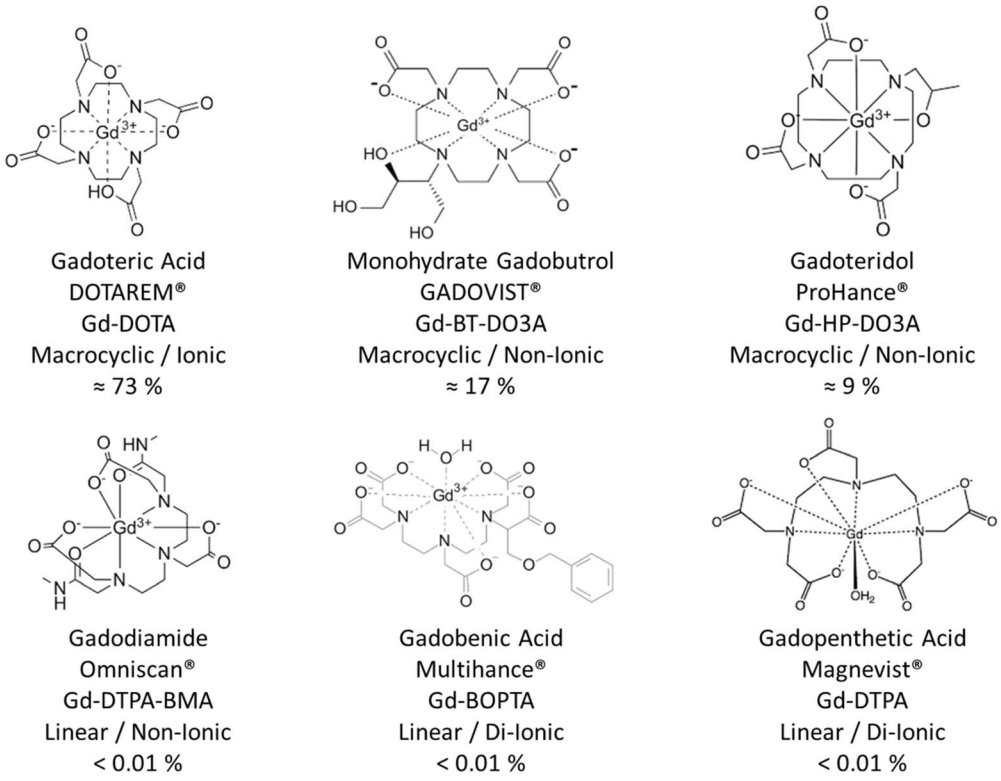

Fig. 1 Structure of the 6 GBCAs currently in use in France with their main characteristics and proportion of use in 2023.

Studies have demonstrated the capability of linear GBCAs to accumulate in the organs, bones or brain tissue of patients treated with linear GBCAs, but to date, there is no evidence of lesions or diseases due to this accumulation of Gd in the human body.[28–30] In surface waters, these complexes have no known health or environmental toxicity. Nevertheless, these complexes can undergo so-called transmetallation mechanisms, whereby the Gd^{3+} ion can be replaced by another metal such as Fe^{3+}, Cu^{2+} or Zn^{2+}.[31–33] Consequently, the release of Gd^{3+} ions can lead to health and environmental risks.[34–37]

Several speciation and quantification methods have been developed to monitor these compounds in the environment. The large majority of these methods involve LC-ICP-MS coupling using a HILIC-type chromatographic column.[14,27,38–43] However, despite good sensitivities (limit of detection (LOD) ranging from 1.3 to 160 ng L^{-1} depending on the compounds and studies) and good resolutions, these methods require the use of large quantities of organic solvents such as acetonitrile or methanol, which are known to be hazardous to health and the environment. In addition, the high presence of organic solvents during ICP-MS measurements results in the formation of a carbon deposit on the sampling and skimming cones, leading to a decrease and instability in signal intensity.[44] To overcome this problem, the addition of gaseous oxygen to the plasma is generally the method used. Another option relies on modification of the sample introduction system (*e.g.* the use of an additional membrane desolvation module). However, both these strategies entail additional analysis costs and instrumental modifications.[45]

Here, a method based on high-pressure ion chromatography coupled with inductively coupled plasma mass spectrometry (HPIC-ICP-MS) is proposed in order to reconcile the factors of green chemistry, cost and efficiency. In concrete terms, the aim of this study is to provide a method using less than 2% organic solvents, which considerably reduces environmental, health and economic impacts, while offering respectable performance in terms of speciation and quantification limits. The present method is also easily transferable to other laboratories that are not equipped to analyse organic solvents by ICP-MS.

2. Materials and methods

2.1. Chemicals

All solutions were prepared using ultrapure water (Milli-Q gradient, Millipore, ρ = 18.2 MΩ cm). Gadolinium-based contrast agents were obtained either in the form of pure compounds by Merck (Darmstadt, Germany) or in the form of commercial injectable solutions provided by the pharmacy of the Lille University Hospital (CHU) or by Bracco Imaging France (Massy, France) in the case of Prohance® (Gd-BT-DO3A). The stock REE multistandard solution (100 mg L^{-1} in 5% HNO_3) was purchased from SCP science (Analytichem, Courtaboeuf, France). Nitric acid (67–69%, ultrapure trace metal grade) and methanol (LC-MS grade) were purchased from VWR international (Fontenay-sous-Bois, France) and Merck, respectively. All other chemicals used in this study were of ACS reagent or analytical grade purity.

2.2. Instrumentation

A high-performance liquid chromatography system (HPLC Bio-inert 1260 Infinity II, Agilent Technologies) equipped with a biocompatible quaternary pump and a metal-free autosampler was used as the separating system. Separation of GBCAs was performed using a Thermo Scientific Dionex IonPac AG7 guard column (10 μm particle diameter, 2 mm internal (i.d.), 50 mm length) coupled with a Thermo Scientific Dionex IonPac AS7 analytical column (10 μm particle diameter, 2 mm i.d., 250 mm length). The volume of injection was set at 25 μL, and the flow rate of the mobile phase was fixed at 450 μL min^{-1}. The outlet of the HPLC column was directly connected to the ICP nebulizer using a 40 cm PEEK capillary tubing (125 μm i.d.). An inductively coupled plasma single quadrupole mass spectrometer (ICP-MS 7900, Agilent Technologies) was used as a detector. The spectrometer was equipped with a PFA concentric nebulizer (0.2 mL min^{-1}), a quartz double pass spray chamber cooled at 2 °C, a quartz torch (2.5 mm i.d.) and nickel cones. X-lenses were selected as an ion optic configuration. High purity He (>99.999%) was used as the collision gas in the octopole reaction system (ORS) in combination with kinetic energy discrimination. In this method, the choice of using ^{158}Gd was based on its higher isotopic abundance (24.8%) than ^{157}Gd (15.7%). The use of He gas not only counterbalances the polyatomic interferences that can interact with ^{158}Gd but also results in a very low background signal close to zero during analysis. Plasma parameters were tuned daily to get optimal signals. Chromatograms were processed using the Agilent MassHunter software by integrating the areas of the peaks. Operating conditions and data acquisition parameters are listed in Table 1.

For the determination of total gadolinium and other REEs, the samples were directly analysed using a single quadrupole Agilent Technologies ICP-MS 7850 quadrupole according to the method previously developed by Trommetter *et al.* (2020).[46]

These total concentrations in water were used to determine the concentrations of anthropogenic Gd (Gd_{anth}), *i.e.* the proportions of Gd originating from anthropogenic sources. Gd_{anth} was determined by the difference between the total Gd measured (Gd_{mes}) and the value of the Gd anomaly (Gd*) according to eqn (1) described by Lerat-Hardy *et al.* (2019).[12] The Gd concentrations are commonly normalized by those in a reference geological value such as EUS (European Shale).[47] This reference takes into account the specificities of Europe' geochemical environment. Gd* therefore corresponds to this normalization, *i.e.* the ratio of Gd_{mes} to the EUS reference of Gd.

Table 1 Optimised ICP-MS settings for HPIC-ICP-MS

RF power (W)	1550
RF matching (V)	1.8
Nebulizer gas (L min^{-1})	1.12
He gas (mL min^{-1})	5
Sample depth (mm)	8
Integration time (s)	0.15
Monitored isotope	^{158}Gd

If Gd* or any other REE* has a value greater than 1, this means that a positive environmental anomaly has been observed.

$$Gd_{anth} = Gd_{mes} - \frac{Gd_{mes}}{Gd^*} = Gd_{mes} - Gd_{mes} \Big/ \frac{Gd_{mes}}{(Nd_{mes} \times 0.2) + (Tb_{mes} \times 0.8)} \quad (1)$$

Nd_{mes} and Tb_{mes} correspond to the total concentrations of neodymium and terbium measured in the samples. As mentioned by Hissler *et al.*, there is no standardized method for calculating Gd_{anth}. The choice of comparisons between Gd and other REEs depends on the specific characteristics of the environment studied in each study. Here, Nd* and Tb* are lower than 1 (data are in the ESI section†), making them good comparators for Gd in this study.[11,12]

3. Results and discussion

3.1. Optimisation of chromatographic parameters

An anion exchange column was used to separate the various Gd-based contrast agents studied. Of the six studied compounds, three are charged. An optimisation of chromatographic parameters was thus essential to obtain optimal separations. Several tests were therefore carried out to define the ideal eluent, the pH of the mobile phase and the elution gradient, with methanol used as the organic solvent. The method was developed by successive analyses of the GBCA standards. Indeed, the analytical development was initially carried out by injecting a mixture of two GBCAs, followed by the addition of a third compound, and so on. In previous studies, ammonium acetate was the most widely used eluent.[24,27,38,39,41,42] In this study, two eluents were tested: ammonium acetate and ammonium nitrate. In our case, ammonium nitrate was found to improve considerably peak resolution and compound separation compared with ammonium acetate.

The elution gradient was also studied. Several tests were carried out both in the presence and absence of MeOH, as well as varying the concentration of NH_4NO_3 in the mobile phase. In all the experiments, the NH_4NO_3 solution is set at pH 7 by

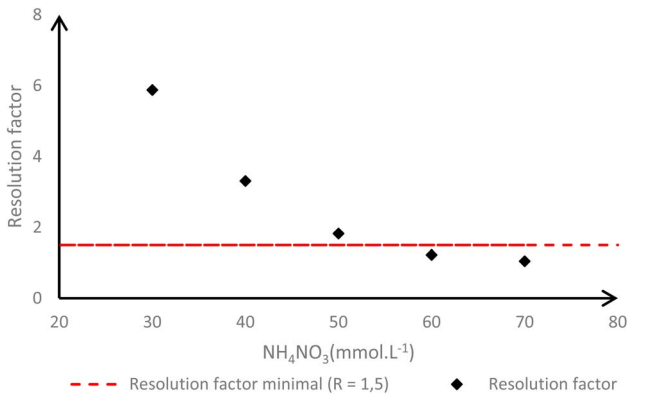

Fig. 2 Influence of NH_4NO_3 concentration on the resolution factor *R*. A threshold value (red line), for which resolution is acceptable, is established in the literature at $R = 1.5$.

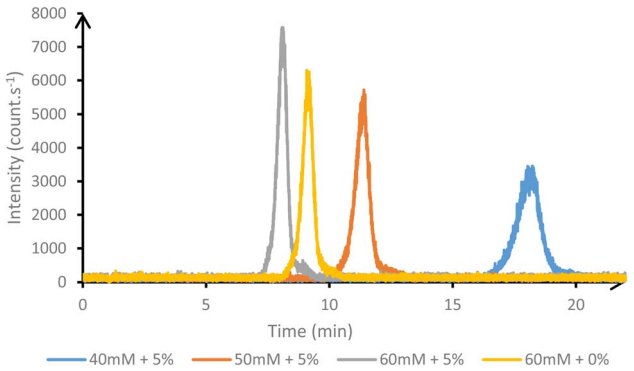

Fig. 3 Influence of NH_4NO_3 (mM) and MeOH (%) mobile phase composition on 1 μg L^{-1} of Gd-BOPTA elution time and peak intensity.

adding NaOH to keep it as close as possible to the pH of surface water.

Preliminary tests were carried out on Gd-DOTA and Gd-DTPA in isocratic mode using only NH_4NO_3 at concentrations ranging from 30 to 60 mM. The aim was to achieve the best possible separation of these two compounds, over the shortest possible analytical run. The resolution factor (eqn (2)) was determined for each condition and is presented in Fig. 2.

$$R = 2 \times \frac{RT_2 - RT_1}{w_1 + w_2} \quad (2)$$

In eqn (2), RT_x corresponds to the retention time of peak $n°x$ and w_x to the width of peak $n°x$ at baseline.

The best compromise between resolution factor and retention time (RT) was attained using an NH_4NO_3 concentration of 50 mM ($R = 1.83$ and 4 min run time).

The addition of MeOH in the NH_4NO_3 eluent (50 mM) was needed to elute Gd-BOPTA in less than 15 min and limit peak broadening. Tests performed on Gd-BOPTA (1 μg L^{-1}) alone were therefore carried out with different concentrations of NH_4NO_3 and MeOH (Fig. 3). A test performed with 40 mM NH_4NO_3 without MeOH was also carried out, but it resulted in a Gd-BOPTA retention time exceeding 20 min. The presence of 5% MeOH in the 40 mM NH_4NO_3 elution solution led to the elution of Gd-BOPTA with a RT = 18.04 min, but with a peak spreading over 4 min. Increasing the NH_4NO_3 concentration resulted in shorter RT (<12 min) and narrower peaks (<2.5 min). For the other GBCAs, the presence of MeOH also contributed to faster elution and allowed the reduction of NH_4NO_3 content in the eluent. Using 2% MeOH and 50 mM NH_4NO_3, Gd-DOTA and Gd-DTPA had RTs of 1.13 min and 2.63 min, respectively, compared to 1.33 min and 4.14 min without MeOH.

Given that 50 mM NH_4NO_3 and 2% MeOH are needed to correctly separate Gd-DOTA and Gd-DTPA in less than 2.5 min, the variation of NH_4NO_3 concentration was tested in a gradient mode from 50 mM to 70 mM, from 2.5 to 8.0 min. The comparison of Gd-BOPTA elution in isocratic and gradient mode is shown in Fig. 4. The use of a gradient mode allows elution of Gd-BOPTA with a higher intensity and a lower retention time and peak spread.

The uncharged GBCAs (Gd-DTPA-BMA; Gd-BT-DO3A; Gd-HP-DO3A) exhibited almost identical RTs, resulting in a single peak for all three compounds tested in a mixture. This is consistent

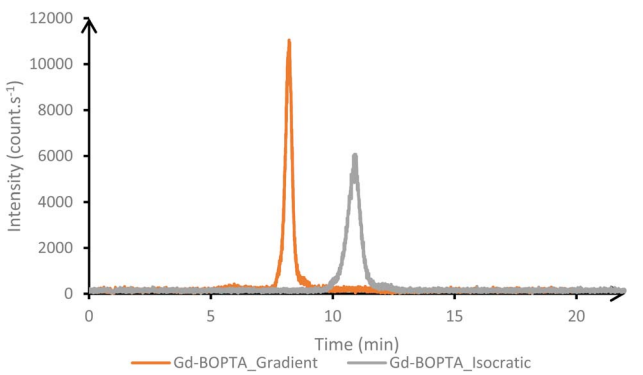

Fig. 4 Influence of the separation mode (gradient or isocratic) on 1 μg L^{-1} of Gd-BOPTA elution time and peak intensity. The mobile phase used in isocratic mode was 50 mM NH_4NO_3 with 2% MeOH. Gradient mode starts with 50 mM NH_4NO_3 and 2% MeOH, increasing to 70 mM from 2.5 to 8.0 min.

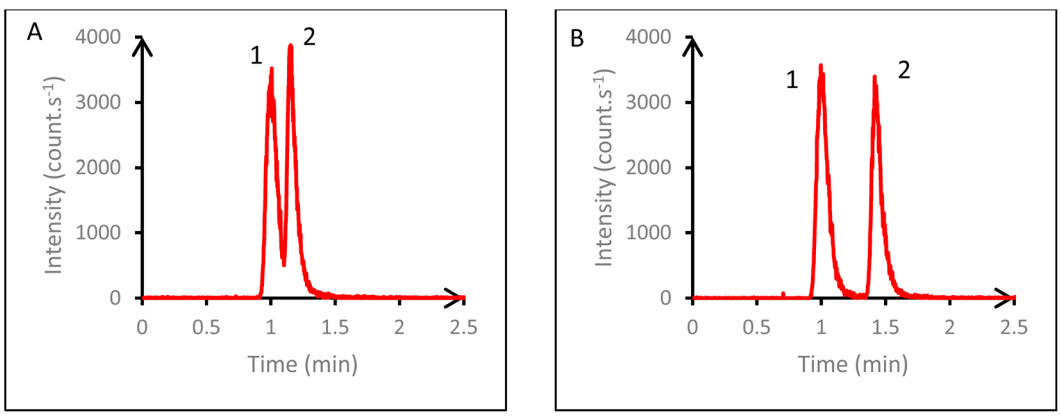

Fig. 5 Influence of the steeper gradient of NH_4NO_3 on 100 ng L^{-1} of Gd-BT-DO3A (Peak 1) and Gd-DOTA (Peak 2) elution time and peak intensity. (A) the gradient starts at 50 mM NH_4NO_3 with 2% MeOH, then increases to 70 mM from 2.5 to 8.0 min. (B) the gradient starts at 20 mM NH_4NO_3 with 2% MeOH and increases to 70 mM from 2.5 to 8.0 min.

Table 2 Optimised chromatographic conditions

Mobile phase eluents			
A = NH_4NO_3 (100 mM/pH 7) B = Ultrapure water C = MeOH			
Operating conditions			
Flow rate (μL min^{-1})			450
Injected volume (μL)			25
Elution gradient			
Time (min)	*A* (%)	*B* (%)	*C* (%)
0	20	78	2
2	20	78	2
2.5	70	28	2
8	70	28	2
8.1	20	78	2
15	20	78	2

with the present ion-exchange column, which can only separate charged compounds. In addition, a steeper gradient of NH_4NO_3 concentration was required in order to separate these uncharged compound peaks from Gd-DOTA. Fig. 5 illustrates the separation of Gd-BT-DO3A and Gd-DOTA (at 100 ng L^{-1}) in gradient modes from 20 mM to 70 mM of NH_4NO_3 (A) and from 50 mM to 70 mM of NH_4NO_3 (B), both increasing from 2.5 to 8.0 min. The peak resolutions achieved were 0.78 and 1.3 under conditions A and B, respectively. Although this resolution factor is not fully acceptable ($R < 1.5$), the two compounds can still be dissociated in this speciation method.

The separation of Gd-BT-DO3A, Gd-BOPTA, Gd-DOTA and Gd-DTPA from a mixed solution at 100 ng L^{-1} under the optimised chromatographic conditions (Table 2) is shown in Fig. 6. The chromatogram shows four peaks with different RTs and intensities. Even if the last compound elutes at 10.5 min, a run time of 15 min is needed to stabilise the column in view of the next injection and also to be able to highlight the presence of new compounds in natural samples. This acceptable run time means that around thirty samples (including the calibration range) can be produced in an 8-hour day.

Calibration curves (up to 500 ng per L Gd) were linear for all compounds at both low and high concentrations (correlation coefficients: ≥0.9995). All the data are provided in the ESI section.† The LOD corresponds to a ratio of compound signal to residual noise upstream of the peak (S/N) equal to 3. The limit of quantification (LOQ) was defined in this study as S/N = 10. These limits determined for each GBCA molecule are presented

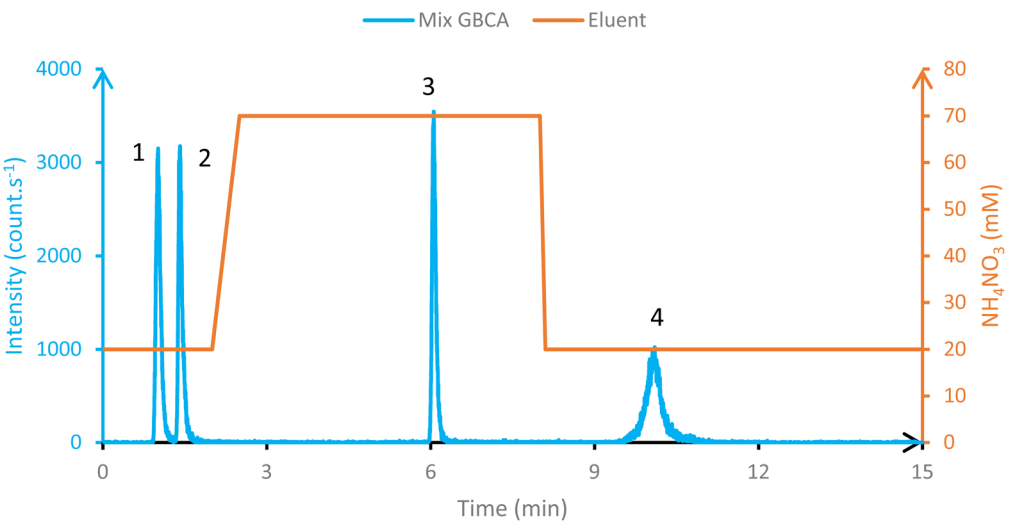

Fig. 6 Chromatogram of a 100 ng L^{-1} mixed solution of Gd-BT-DO3A, Gd-DOTA, Gd-DTPA and Gd-BOPTA under the optimised conditions. Peak assignment: 1, Gd-BT-DO3A; 2, Gd-DOTA; 3, Gd-DTPA; 4, Gd-BOPTA.

Table 3 LOD and LOQ of GBCAs evaluated in this study compared to other studies

	LOD and LOQ in ng L^{-1} of Gd											
	Gd-BT-DO3A		Gd-HP-DO3A		Gd-DTPA-BMA		Gd-DOTA		Gd-DTPA		Gd-BOPTA	
Reference	LOD	LOQ	LOD	LOQ	LOD	LOQ	LOD	LOQ	LOD	LOQ	LOD	LOQ
This work	2	4	2	4	2	8	2	4	4	8	5	30
Macke *et al.* (2021)[18]	1.73	5.98	2.2	7.08	—	—	1.73	5.98	2.2	7.39	2.99	10.22
Okabayashi *et al.* (2021)[42]	6.6	22	22	72	3.7	13	5.9	20	3.4	11	—	—
Birka *et al.* (2013)[14]	13	44.03	—	—	—	—	16	58.18	14	48.75	—	—

Table 4 Main characteristics of the methods used in the different studies

Reference	Separation mode	Detection method	Preconcentration/dilution process
This work	IC	ICP-QMS	None
Macke *et al.* (2021)[18]	IC	TQ ICP-MS	prepFAST M5
Okabayashi *et al.* (2021)[42]	HILIC	ICP-QMS	None
Birka *et al.* (2013)[14]	HILIC	Q ICP-MS	None

in ng L^{-1} of Gd (Table 3). These values have a reproducibility of around 5%. The obtained values show that the present method is as sensitive as, or even more sensitive than, previous methods found in the literature (Table 3 and 4).[14,18,42]

In the environment, Gd concentrations range from < 1 ng L^{-1} to several hundred ng L^{-1} in surface waters (rivers), and can even reach the μg L^{-1} level in WWTPs.[14,15,21,43] In this context, the analytical method developed here, with its low LOD and LOQ, appears to be suitable for environmental studies. In addition, triplicate measurements of the calibration range standards were carried out in two analyses on two different days. This experiment showed that the error did not exceed 3% of the concentration.

3.2. pH-dependent stability of GBCAs

GBCA stability was tested using buffer solutions at different pH values (from 4.0 to 10.0). Buffer solutions were prepared from KH_2PO_4 (0.01 M) and K_2HPO_4 (0.01 M). The standard solutions were spiked at 1 μg L^{-1} in these buffer solutions and immediately analysed by HPIC-ICP-MS. The influence of the pH on the response of these compounds is illustrated in Fig. 7. With the exception of Gd-DTPA-BMA, the compounds were found to be stable between pH 5 and pH 9. At pH 10, most compounds undergo a 10 to 20% decrease in their initial concentration. At pH 4, a decrease of around 77%, 81% and 93% was observed for Gd-BOPTA, Gd-DTPA and Gd-DTPA-BMA, respectively. The latter was found very sensitive to changes of pH (Fig. 7). One hypothesis would be the possible hydrolysis of the amide functions of this compound, leading to a structural modification of the ligand and a possible release of free Gd^{3+} ions.

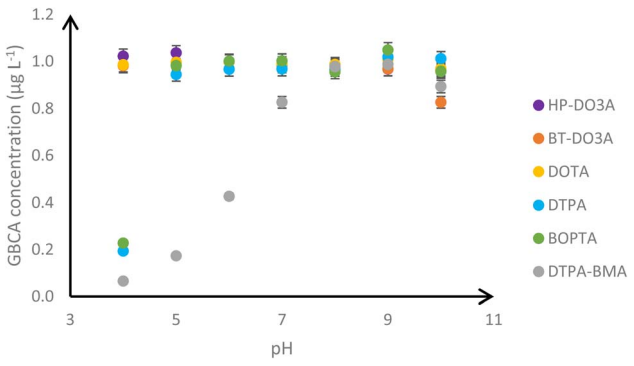

Fig. 7 Influence of the pH on the concentration of GBCA standards doped to 1 μg L^{-1} initially. These values have a reproducibility of around 3%.

Concerning RTs (ESI section†), no significant influence of pH was observed for Gd-DTPA-BMA or Gd-HP-DO3A, whose RTs remained stable at 0.99 min and 1.00 min, respectively. At pH 10, Gd-DTPA and Gd-BOPTA presented a slight decrease in RT (from 6.08 min to 6.00 min at pH 10 and from 10.2 min to 10.1 min at pH 10, respectively), whereas Gd-BT-DO3A exhibited a slightly increasing RT (from 1.00 min to 1.04 min at pH 10). Gd-DOTA was stable from pH 5 to pH 9 at around 1.40 min, but increased slightly at pH 4 (1.45 min) and decreased slightly at pH 10 (1.33 min).

In light of these observations, with the exception of Gd-DTPA-BMA, analysis of the GBCAs studied raises no problems over a pH range of 5 to 9. By contrast, pH 4 and pH 10 seem to contribute to a structural modification of the GBCAs. Hypotheses can be studied, in particular, on the release of Gd^{3+} ions, especially at an acidic pH where the carboxylate functions of the ligands could be protonated. In addition, the slight changes of RTs observed at pH 4 and pH 10 are probably related to a variation in the affinity of these compounds with the stationary phase of the column. Further tests are needed to investigate these hypotheses, but these are beyond the scope of this paper.

In any case, for natural samples, the pH of the water, although it may vary slightly, should have no impact on the stability of the GBCAs.

3.3. Quantification of Gd-based contrast agents in surface water

In order to validate the present method for surface water analysis, two samples were taken from the Marque River at Villeneuve d'Ascq (France) and another one directly from the discharge of the WWTP into this small river during a sampling campaign carried out on 15th October 2024. The Marque River rises in Mons-en-Pévèle and flows into the Deûle at Marquette-lez-Lille after 32 km. In addition, eight WWTPs discharge their effluent into the Marque River or one of its 22 tributaries.[48] Sampling point P1 corresponds to the point upstream of the WWTP into the Marque River, approximately 50 m from the discharge. Point P2 corresponds to the direct discharge of the WWTP into the Marque River, and P3 is located downstream at 1300 m of the WWTP (Fig. 8). All samples were collected using a telescopic pole and 500 mL fluoropolymer (FEP) bottles washed with acid beforehand. For each sample, the bottle was

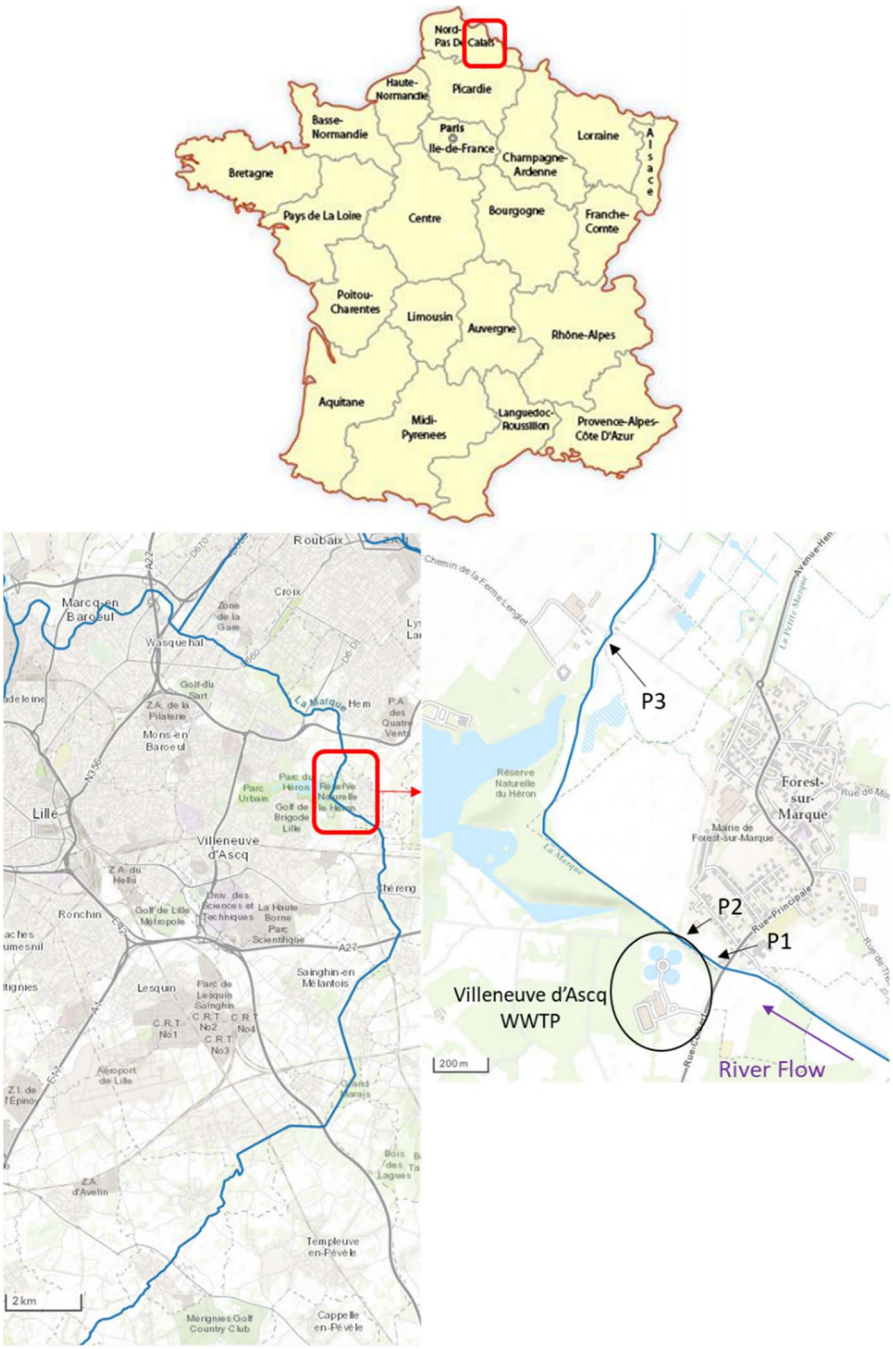

Fig. 8 Location of the sampling points in the Marque River.

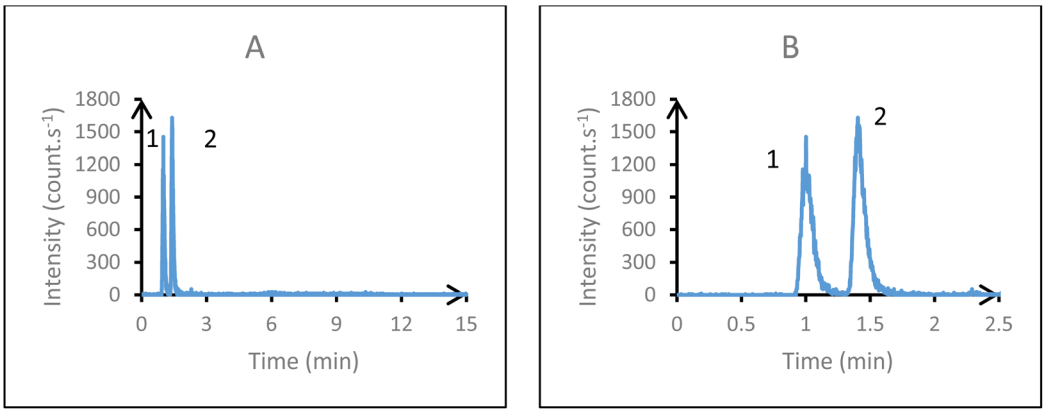

Fig. 9 Chromatogram of sampled surface water at P1 ((A): original chromatogram; (B): enlarged view of (A)). Peak assignment: (1) uncharged GBCA; (2) Gd-DOTA.

rinsed three times with water from the sampling point. For total metal analysis, water samples were immediately filtered on site using 0.45 µm cellulose acetate filters and acidified to 2% v/v with ultrapure nitric acid (HNO_3). For the GBCA speciation analysis, the samples were filtered as above but were not acidified. All samples were stored at 4 °C in polypropylene vials before the analyses were carried out the same day.

Acidified samples were first analysed by ICP-MS to obtain total REE concentrations. These concentrations were used to highlight the consequent Gd anomalies through REE patterns normalized to the European Shale (EUS) reference standards.[12] Total REE concentrations and REE patterns are presented in the ESI section.†

Non-acidified samples were analysed by HPIC-ICP-MS for GBCA speciation. Fig. 9–11 show the chromatograms obtained for each sample, with enlarged views of the first two minutes of the run.

For each sampling point, only two peaks were observed, the first one corresponding to uncharged GBCAs and the second one to Gd-DOTA. These peaks were assigned by comparing the RTs of standardised commercial solutions of GBCAs. The other compounds were not observed, which can be explained by their very limited use in France. Concentrations were determined by integration of the peaks after calibration curves using standards. The proportion of Gd_{anth} was calculated according to eqn (1) from the total concentrations of Gd and the other rare earth elements in the samples. Several hypotheses can be made concerning the composition of peak no. 1 (Fig. 9–11). In view of the use of GBCAs in France, there is a high probability that this peak corresponds essentially to a mixture of Gd-BT-DO3A (17% of use in France) and Gd-HP-DO3A (9%), with a majority of Gd-BT-DO3A. In addition, these two compounds have a similar response and therefore a close calibration slope. Indeed, only a 4% error in concentration was found between these two calibrations. Thus, in view of the proportion used in France (17%) and the low percentage of error in concentration (4%) between these two calibrations, for our study, the calibration range for Gd-BT-DO3A is sufficient to approximate the values of the peak no. 1. The main results are shown in Table 5.

A significant difference was observed between the sampling points. Indeed, a lower concentration of GBCA was obtained upstream of the WWTP (P1 – 95 ng L^{-1}) compared to the WWTP's discharge (P2 – 507 ng L^{-1}) and downstream (P3 – 159 ng L^{-1}). The presence of these compounds in P1 is not

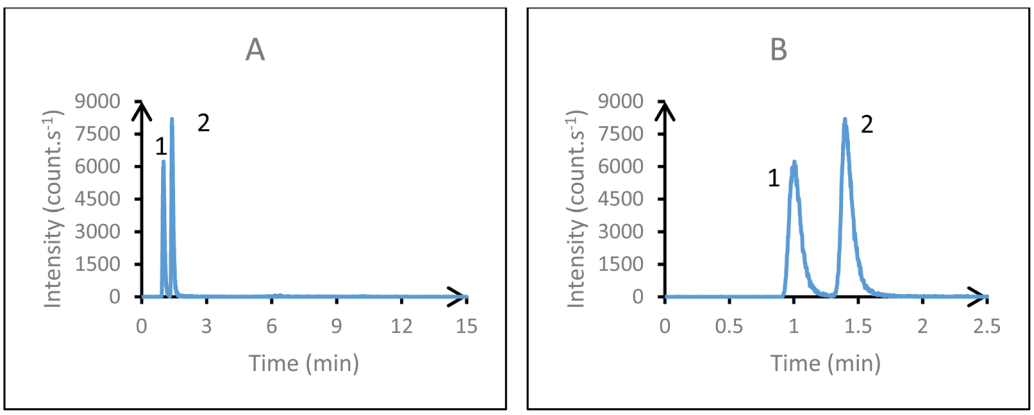

Fig. 10 Chromatogram of WWTP's discharge at P2 ((A): original chromatogram; (B): enlarged view of (A)). Peak assignment: (1) uncharged GBCA; (2) Gd-DOTA.

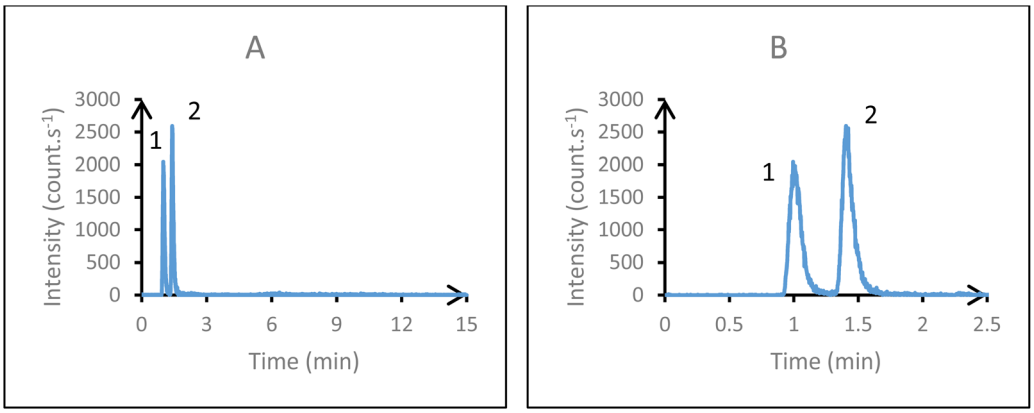

Fig. 11 Chromatogram of sampled surface water at P3 ((A): original chromatogram; (B): enlarged view of (A)). Peak assignment: (1) uncharged GBCA; (2) Gd-DOTA.

Table 5 Concentrations of GBCAs found (ng L^{-1} of Gd) in the stations P1, P2 and P3 measured by HPIC-ICP-MS and total Gd concentrations in these samples measured by ICP-MS. These values have a reproducibility of around 5%[a]

		P1	P2	P3
Uncharged-GBCA	(ng L^{-1})	42	227	72
Gd-DOTA	(ng L^{-1})	53	279	87
∑GBCA	(ng L^{-1})	95	507	159
Total Gd	(ng L^{-1})	101	522	172
Gd_{anth}	(ng L^{-1})	99	521	169
$\%Gd_{anth}$	(%)	98	99	98

[a] Gd_{Anth} is therefore clearly quite exclusively linked to the presence of GBCAs. From Table 5, it can be seen that Gd-uncharged and Gd-DOTA correspond to the majority of the Gd found in the Marque River, with ≈42% and ≈52% of the total Gd, respectively. Furthermore, only Gd-DOTA and Gd-uncharged were detected, which is in accordance with the use of these compounds in France.

surprising since other discharges of WWTPs upstream correspond to a total nominal capacity of 46 320 p.e. By comparison, the WWTP of Villeneuve d'Ascq has a nominal capacity of over 151 000 p.e. A decrease in GBCA concentrations was observed between the discharge (P2) and the downstream's point (P3) of the WWTP (69% loss for uncharged-GBCA and for Gd-DOTA). This is explained by dilution of the discharge into the river and is supported by the profile of other more conventional tracers (*i.e.* chloride ions, nitrate ions, conductivity…), which exhibit the same trend between these three points. To this end, a statistical comparison (least squares method), carried out on 8 other tracers plus gadolinium, demonstrated the latter's conservative behaviour in our study area (ESI section†).[1,49] In addition, the total Gd concentration corresponds to 98% of Gd_{anth} upstream, 99% in the discharge and 98% downstream of the WWTP (Table 5).

4. Conclusion

In this study, a new HPIC-ICP-MS method allowing the speciation and the quantification of GBCAs in water has been developed. This method has been successfully applied to real environmental samples. This new analytical method, with low environmental impact, offers good performance in terms of detection and quantification limits (LOD = 2–5 ng L^{-1} of Gd; LOQ = 4–30 ng L^{-1} of Gd), and is therefore perfectly suited to environmental studies. It also offers reasonable analysis times (15 min) and does not require any instrumental modifications. Nevertheless, one point remains to be developed: the speciation of uncharged GBCAs. For the moment, the quantity of uncharged GBCAs is determined on the basis of the calibration of Gd-BT-DO3A (the uncharged GBCA most widely used in France). Although the error associated with this approximation is minimal, it would be desirable in the future to have speciation for all three uncharged GBCAs. In addition, this method could be further optimised, particularly if a higher analysis rate is required. Indeed, the gradient can be further improved to reduce the analysis time. It should also be possible to reduce the injection volumes by reducing the column size.

Analyses of natural samples have revealed the presence of GBCA pollution in surface waters in northern France, corresponding to 93 and 98% of Gd_{anth}, depending on where the samples were taken. In addition, the WWTP of Villeneuve d'Ascq discharges increases the concentrations of these compounds that behave like other conventional conservative tracers. Finally, this method could therefore provide valuable information for monitoring and controlling this emerging pollution in countries that use GBCAs for MRI.

Data availability

For this article, data are available upon request from the authors.

Author contributions

The manuscript was written through contributions of all authors, and all authors have given approval to the final version of the manuscript.

Conflicts of interest

There are no conflicts to declare.

Acknowledgements

HPIC-ICP-MS measurements were performed on the Chevreul Institute Platform (U-Lille/CNRS). The Region Hauts-de-France and the French government are warmly acknowledged for the co-funding of this apparatus. The authors thank the Région Hauts-de-France, the Ministère de l'Enseignement Supérieur et de la Recherche and the European Fund for Regional Economic Development for their financial support to the CPER ECRIN program. The Artois Picardie French Water Agency and the Region Hauts-de-France are also acknowledged for the PhD funding of Manon Dalla Costa.

References

1 G. Trommetter. Développements analytiques et d'échantillonneurs passifs appliqués aux terres rares et platinoïdes : application aux systèmes aquatiques anthropisés [Internet] [These de doctorat]. Université de Lille (2018-2021); 2020 [cited 2024 Mar 20], available from: https://theses.fr/2020LILUR051.

2 I. Lim, C. Sun, J. H. Lee, J. Kim, S. Lee, H. Sim, *et al.*, Seasonal variations of dissolved rare earth elements and anthropogenic gadolinium in the highly urbanized river basin, Busan, Korea., *Estuarine, Coastal Shelf Sci.*, 2023, **288**, 108359.

3 H. Elderfield and M. J. Greaves, The rare earth elements in seawater, *Nature*, 1982, **296**, 214–219.

4 M. Bau and P. Dulski, anthropogenic origin of positive gadolinium anomalies in river waters, *Earth Planet. Sci. Lett.*, 1996, **143**(1–4), 245–255.

5 H. Bassett, A. Silverman, K. A. Jensen, G. H. Cheesman, J. Bénard, N. Bjerrum, *et al.*, Nomenclature of Inorganic Chemistry, *J. Am. Chem. Soc.*, 1960, **82**(21), 5523–5544.

6 E. Perrat. Impacts environnementaux des agents de contraste à base de Gadolinium : situation locale, approche cellulaire et *in vivo* [Internet] [These de doctorat]. Université de Lorraine, 2017 [cited 2024 Mar 20]. available from: https://theses.fr/2017LORR0370.

7 S. Massari and M. Ruberti, Rare earth elements as critical raw materials: Focus on international markets and future strategies, *Resour. Policy*, 2013, **38**(1), 36–43.

8 B. Zhou, Z. Li and C. Chen, Global Potential of Rare Earth Resources and Rare Earth Demand from Clean Technologies, *Minerals*, 2017, **7**(11), 203.

9 X. Wang, M. Yao, J. Li, K. Zhang, H. Zhu and M. Zheng, China's Rare Earths Production Forecasting and Sustainable Development Policy Implications, *Sustainability*, 2017, **9**, 1003.

10 Z. Zhu, C. Q. Liu, Z. L. Wang, X. Liu and J. Li, Rare earth elements concentrations and speciation in rainwater from Guiyang, an acid rain impacted zone of Southwest China, *Chem. Geol.*, 2016, **442**, 23–34.

11 C. Hissler, R. Hostache, J. F. Iffly, L. Pfister and P. Stille, Anthropogenic rare earth element fluxes into floodplains: Coupling between geochemical monitoring and hydrodynamic sediment transport modelling, *C. R. Geosci.*, 2015, **347**(5), 294–303.

12 A. Lerat-Hardy, A. Coynel, L. Dutruch, C. Pereto, C. Bossy, T. Gil-Diaz, *et al.*, Rare Earth Element fluxes over 15 years into a major European Estuary (Garonne-Gironde, SW France): Hospital effluents as a source of increasing gadolinium anomalies, *Sci. Total Environ.*, 2019, **656**, 409–420.

13 W. Gwenzi, L. Mangori, C. Danha, N. Chaukura, N. Dunjana and E. Sanganyado, Sources, behaviour, and environmental and human health risks of high-technology rare earth elements as emerging contaminants, *Sci. Total Environ.*, 2018, **636**, 299–313.

14 M. Birka, C. A. Wehe, L. Telgmann, M. Sperling and U. Karst, Sensitive quantification of gadolinium-based magnetic resonance imaging contrast agents in surface waters using hydrophilic interaction liquid chromatography and inductively coupled plasma sector field mass spectrometry, *J. Chromatogr. A*, 2013, **1308**, 125–131.

15 A. Laczovics, I. Csige, S. Szabó, A. Tóth, F. K. Kálmán, I. Tóth, *et al.*, Relationship between gadolinium-based MRI contrast agent consumption and anthropogenic gadolinium in the influent of a wastewater treatment plant, *Sci. Total Environ.*, 2023, **877**, 162844.

16 I. A. Wysocka, A. M. Rogowska and P. Kostrz-Sikora, Investigation of anthropogenic gadolinium in tap water of polish cities: Gdańsk, Kraków, Warszawa, and Wrocław, *Environ. Pollut.*, 2023, **323**, 121289.

17 P. Louis, A. Messaoudene, H. Jrad, B. A. Abdoul-Hamid, D. A. L. Vignati and M. N. Pons, Understanding Rare Earth Elements concentrations, anomalies and fluxes at the river basin scale: The Moselle River (France) as a case study, *Sci. Total Environ.*, 2020, **742**, 140619.

18 M. Macke, C. D. Quarles, M. Sperling and U. Karst, Fast and automated monitoring of gadolinium-based contrast agents in surface waters, *Water Res.*, 2021, **207**, 117836.

19 J. Rogowska, E. Olkowska, W. Ratajczyk and L. Wolska, Gadolinium as a new emerging contaminant of aquatic environments, *Environ. Toxicol. Chem.*, 2018, **37**(6), 1523–1534.

20 Assurance Maladie. L'Assurance Maladie. 2024 cited 2024 Jul 11, Médicaments délivrés par les pharmacies de ville par type de prescripteur – Medic'AM – 2015 à 2024, available from: https://www.assurance-maladie.ameli.fr/etudes-et-donnees/medicaments-type-prescripteur-medicam.

21 K. Inoue, M. Fukushi, S. K. Sahoo, N. Veerasamy, A. Furukawa, S. Soyama, *et al.*, Measurements and future projections of Gd-based contrast agents for MRI exams in wastewater treatment plants in the Tokyo metropolitan area, *Mar. Pollut. Bull.*, 2022, **174**, 113259.

22 I. E. Oluwasola, A. L. Ahmad, N. F. Shoparwe and S. Ismail, Gadolinium based contrast agents (GBCAs): Uniqueness, aquatic toxicity concerns, and prospective remediation, *J. Contam. Hydrol.*, 2022, **250**, 104057.

23 J. P. Goullé, E. Saussereau, L. Mahieu, D. Cellier, J. Spiroux and M. Guerbet, Importance of anthropogenic metals in hospital and urban wastewater: its significance for the environment, *Bull. Environ. Contam. Toxicol.*, 2012, **89**(6), 1220–1224.
24 L. Telgmann, M. Sperling and U. Karst, Determination of gadolinium-based MRI contrast agents in biological and environmental samples: A review, *Anal. Chim. Acta*, 2013, **764**, 1–16.
25 R. Brünjes and T. Hofmann, Anthropogenic gadolinium in freshwater and drinking water systems, *Water Res.*, 2020, **182**, 115966.
26 J. M. Zabrecky, X. M. Liu, Q. Wu and C. Cao, Evidence of Anthropogenic Gadolinium in Triangle Area Waters, North Carolina, USA, *Water*, 2021, **13**(14), 1895.
27 M. Horstmann, R. G. de Vega, D. P. Bishop, U. Karst, P. A. Doble and D. Clases, Determination of gadolinium MRI contrast agents in fresh and oceanic waters of Australia employing micro-solid phase extraction, HILIC-ICP-MS and bandpass mass filtering, *J. Anal. At. Spectrom.*, 2021, **36**(4), 767–775.
28 C. M. Costelloe, B. Amini and J. E. Madewell, Risks and Benefits of Gadolinium-Based Contrast-Enhanced MRI, *Seminars Ultrasound, CT MRI*, 2020, **41**(2), 170–182.
29 N. Iyad, S. M. Ahmad, S. G. Alkhatib and M. Hjouj, Gadolinium contrast agents- challenges and opportunities of a multidisciplinary approach: Literature review, *Eur. J. Radiol. Open*, 2023, **11**, 100503.
30 A. G. Winterstein, T. N. Thai, S. Nduaguba, N. E. Smolinski, X. Wang, L. Sahin, *et al.*, Risk of fetal or neonatal death or neonatal intensive care unit admission associated with gadolinium magnetic resonance imaging exposure during pregnancy, *Am. J. Obstet. Gynecol.*, 2023, **228**(4), 465.e1–465.e11.
31 M. Rabiet, M. Letouzet, S. Hassanzadeh and S. Simon, Transmetallation of Gd-DTPA by Fe3+, Cu2+ and Zn2+ in water: Batch experiments and coagulation–flocculation simulations, *Chemosphere*, 2014, **95**, 639–642.
32 A. Bichler, C. Muellegger, R. Brünjes and T. Hofmann, Quantification of river water infiltration in shallow aquifers using acesulfame and anthropogenic gadolinium, *Hydrol. Processes*, 2015, **30**, 1742–1756.
33 R. Brünjes, A. Bichler, P. Hoehn, F. T. Lange, H. J. Brauch and T. Hofmann, Anthropogenic gadolinium as a transient tracer for investigating river bank filtration, *Sci. Total Environ.*, 2016, **571**, 1432–1440.
34 G. Trapasso, S. Chiesa, R. Freitas and E. Pereira, What do we know about the ecotoxicological implications of the rare earth element gadolinium in aquatic ecosystems?, *Sci. Total Environ.*, 2021, **781**, 146273.
35 S. Szabó, G. Zavanyi, G. Koleszár, D. del Castillo, V. Oláh and M. Braun, Phytoremediation, recovery and toxic effects of ionic gadolinium using the free-floating plant *Lemna gibba*, *J. Hazard. Mater.*, 2023, **458**, 131930.
36 V. F. Scurtu, D. Clapa, L. F. Leopold, F. Ranga, D. Iancu Ştefania, A. I. Cadiş, *et al.*, Gadolinium Accumulation and Toxicity on *In Vitro* Grown Stevia rebaudiana: A Case-Study on Gadobutrol, *Int. J. Mol. Sci.*, 2022, **23**(19), 11368.
37 Z. Liu, C. Guo, P. Tai, L. Sun and Z. Chen, The exposure of gadolinium at environmental relevant levels induced genotoxic effects in *Arabidopsis thaliana* (L.), *Ecotoxicol. Environ. Saf.*, 2021, **215**, 112138.
38 M. Birka, J. Roscher, M. Holtkamp, M. Sperling and U. Karst, Investigating the stability of gadolinium based contrast agents towards UV radiation, *Water Res.*, 2016, **91**, 244–250.
39 S. Feng, S. Shen, Y. Yao, M. Liang, Y. Chen and H. Liu, Comparison of different analytical methods for speciation of seven gadolinium-based magnetic resonance imaging contrast agents and the applications in wastewater and whole blood, *J. Sep. Sci.*, 2023, **46**(4), e2200575.
40 J. Künnemeyer, L. Terborg, B. Meermann, C. Brauckmann, I. Möller, A. Scheffer, *et al.*, Speciation analysis of gadolinium chelates in hospital effluents and wastewater treatment plant sewage by a novel HILIC/ICP-MS method, *Environ. Sci. Technol.*, 2009, **43**(8), 2884–2890.
41 U. Lindner, J. Lingott, S. Richter, W. Jiang, N. Jakubowski and U. Panne, Analysis of gadolinium-based contrast agents in tap water with a new hydrophilic interaction chromatography (ZIC-cHILIC) hyphenated with inductively coupled plasma mass spectrometry, *Anal. Bioanal. Chem.*, 2015, **407**(9), 2415–2422.
42 S. Okabayashi, L. Kawane, N. Y. Mrabawani, T. Iwai, T. Narukawa, M. Tsuboi, *et al.*, Speciation analysis of Gadolinium-based contrast agents using aqueous eluent-hydrophilic interaction liquid chromatography hyphenated with inductively coupled plasma-mass spectrometry, *Talanta*, 2021, **222**, 121531.
43 L. Schlatt, A. Köhrer, C. Factor, P. Robert, M. Rasschaert, M. Sperling, *et al.*, Mild Dissolution/Recomplexation Strategy for Speciation Analysis of Gadolinium from MR Contrast Agents in Bone Tissues by Means of HPLC-ICP-MS, *Anal. Chem.*, 2021, **93**(33), 11398–11405.
44 A. Leclercq, A. Nonell, J. L. Todolí Torró, C. Bresson, L. Vio, T. Vercouter, *et al.*, Introduction of organic/hydro-organic matrices in inductively coupled plasma optical emission spectrometry and mass spectrometry: A tutorial review. Part I. Theoretical considerations, *Anal. Chim. Acta*, 2015, **885**, 33–56.
45 A. Leclercq, A. Nonell, J. L. Todolí Torró, C. Bresson, L. Vio, T. Vercouter, *et al.*, Introduction of organic/hydro-organic matrices in inductively coupled plasma optical emission spectrometry and mass spectrometry: A tutorial review. Part II. Practical considerations, *Anal. Chim. Acta*, 2015, **885**, 57–91.
46 G. Trommetter, D. Dumoulin and G. Billon, Direct determination of rare earth elements in natural water and digested sediment samples by inductively coupled plasma quadrupole mass spectrometry using collision cell, *Spectrochim. Acta, Part B*, 2020, **171**, 105922.
47 M. Bau, K. Schmidt, A. Pack, V. Bendel and D. Kraemer, The European Shale: An improved data set for normalisation of rare earth element and yttrium concentrations in

environmental and biological samples from Europe, *Appl. Geochem.*, 2018, **90**, 142–149.

48 A. Ivanovsky, J. Criquet, D. Dumoulin, C. Alary, J. Prygiel, L. Duponchel, *et al.*, Water quality assessment of a small peri-urban river using low and high frequency monitoring, *Environ. Sci.: Processes Impacts*, 2016, **18**(5), 624–637.

49 D. Guinoiseau, P. Louvat, G. Paris, J. B. Chen, B. Chetelat, V. Rocher, *et al.*, Are boron isotopes a reliable tracer of anthropogenic inputs to rivers over time?, *Sci. Total Environ.*, 2018, **626**, 1057–1068.